Journal of Materials Chemistry A

COMMUNICATION

View Article Online
View Journal

Cite this: DOI: 10.1039/c5ta02380g

A subtractive approach to molecular engineering of dimethoxybenzene-based redox materials for non-aqueous flow batteries†

Received 1st April 2015
Accepted 18th June 2015

DOI: 10.1039/c5ta02380g

www.rsc.org/MaterialsA

Jinhua Huang,‡[ab] Liang Su,‡[ac] Jeffrey A. Kowalski,[ac] John L. Barton,[ac] Magali Ferrandon,[ab] Anthony K. Burrell,[ab] Fikile R. Brushett*[ac] and Lu Zhang*[ab]

The development of new high capacity redox active materials is key to realizing the potential of non-aqueous redox flow batteries (RFBs). In this paper, a series of substituted 1,4-dimethoxybenzene based redox active molecules have been developed *via* a subtractive design approach. Five molecules have been proposed and developed by removing or reducing the bulky substituent groups of DBBB (2,5-di-*tert*-butyl-1,4-bis(2-methoxyethoxy)benzene), a successful over-charge protection material for lithium-ion batteries. Of these derivatives, 2,3-dimethyl-1,4-dimethoxybenzene (23DDB) and 2,5-dimethyl-1,4-dimethoxybenzene (25DDB) are particularly promising as they demonstrate favorable electrochemical characteristics at gravimetric capacities (161 mA h g^{-1}) that approach the stability limit of chemically reversible dimethoxybenzene based structures. Diffusivity, solubility, and galvanostatic cycling results indicate that both 23DDB and 25DDB molecules have promise for non-aqueous RFBs.

The demand for stationary electrical energy storage systems is forecast to grow significantly in the coming years, due to their potential to facilitate the widespread integration of renewable, non-dispatchable energy sources, such as solar and wind, on the grid, and to provide for a range of services that include deferral of infrastructure investments, grid stabilization, and resiliency through back-up power.[1–3] Redox flow batteries (RFBs) have the potential to meet the challenging technical and economic requirements for cost-effective storage deployment.[4] However, significant improvements in the performance, durability, and manufacturing of current RFB technologies are required to meet system cost targets established by the U.S. Department of Energy.[5,6] To this end, significant research activities have been focused on lowering system costs and improving energy densities through high-performance electro-reactors,[7,8] new electrolyte formulations,[2] and novel tailored redox molecules.[9]

While the vast majority of RFB chemistries are based on aqueous couples, of late, increasing efforts have focused on exploring the non-aqueous design space. Transitioning from aqueous to non-aqueous electrolytes offers a wider window of electrochemical stability that enables operation at higher cell voltages (>4 V).[10] Further, a greater selection of redox materials may be available due to the wider solvent stability window and the variety of non-aqueous solvents. Together these benefits promise to reduce the cost of energy and potentially enable high-energy small-footprint storage devices. However, the increased cost and lower ionic conductivity of non-aqueous electrolytes, as compared to their aqueous counterparts, places design constraints on active materials including high gravimetric charge capacity (~180 mA h g^{-1}), high solubility (>0.8 kg kg^{-1}) and high cell voltage (>3 V) to meet aggressive cost targets (low $100's per useable kW h).[4] Note that the gravimetric charge capacity refers to the intrinsic capacity of the candidate active materials rather than the capacity of the flow battery itself. Developing redox chemistries to meet these materials-level targets is key to realizing cost-effective non-aqueous RFBs. Here we seek to identify pathways to redox compounds in line with these material requirements through careful pruning of stable redox structures engineered for different energy applications.

First proposed in the 1980s, small electroactive molecules have been employed as redox shuttles to improve lithium (Li)-ion cell safety, specifically overcharge protection. Through advances in molecular engineering and electrolyte formulation, a number of redox-active organic molecules have demonstrated stable performance for 100s of overcharge cycles with various Li-ion cell chemistries. Many of the materials developed and knowledge gained in this field over the past 30 years can be

[a]*Joint Center for Energy Storage Research, Argonne National Laboratory, Lemont, IL 60439, USA. E-mail: brushett@mit.edu; luzhang@anl.gov*

[b]*Chemical Sciences and Engineering Division, Argonne National Laboratory, Lemont, IL 60439, USA*

[c]*Department of Chemical Engineering, Massachusetts Institute of Technology, Cambridge, MA 02139, USA*

† Electronic supplementary information (ESI) available: Acronyms of chemicals, experimental section, commercial source of DB, and MDB, synthetic procedure of 23DDB, 25DDB and 26DDB, cyclic voltammograms of MDB, 26DDB, Randle–Sevcik plots of DBBB, 25DDB, 23DDB, and ^{1}H NMR and ^{13}C NMR spectra of 23DDB, 25DDB, 26DDB. See DOI: 10.1039/c5ta02380g

‡ These authors contribute equally to this work.

directly leveraged to guide the design of high performance active materials for non-aqueous RFBs. However, differences in the material requirements between overcharge protection molecules in Li-ion batteries and redox compounds in non-aqueous RFBs lead to several new challenges. First, in flow batteries, the organic molecules serve as energy-bearing species requiring high charge carrier concentrations to enable high energy storage. Second, in flow batteries, the active species must be stable in their charged state for hours to days. In comparison, overcharge protection materials function as electrolyte additives and thus have lower solubility requirements. Also, they remain charged for the time period required to traverse the separator (~25–50 μm thickness) within an enclosed cell (generally, on the order of seconds).

Here, we aim to re-engineer a successful overcharge protection material, 2,5-di-*tert*-butyl-1,4-bis(2-methoxyethoxy)benzene (DBBB, Fig. 1), for non-aqueous RFB applications.[11,12] In particular, we modify the substituent groups around the 1,4-alkoxybenzene redox center with the overarching goal of increasing molecular capacity and imparting other favorable properties (*e.g.*, increased solubility). Based on DBBB, we have previously developed a series of room-temperature liquid redox active compounds by modifying the polyethylene oxide (PEO) side chains of the dimethoxy-di-*tert*-butyl-benzene based redox structure.[13–16] However, the storage capacities of these compounds are lower than desired ($\leq$100 mA h g^{-1}). In this contribution, we report on the electrochemical characterization of two promising dimethoxybenzene derivatives, 2,3-dimethyl-1,4-dimethoxybenzene (23DDB) and 2,5-dimethyl-1,4-dimethoxybenzene (25DDB), as high-potential redox active molecules for non-aqueous RFBs. As compared to DBBB, these compounds demonstrated increased gravimetric capacity and solubility without sacrificing electrochemical performance. Furthermore, high gravimetric capacity may enable additive molecular design strategies to be employed to enhance stability.

Motivated by the favorable electrochemical properties but low gravimetric capacity of DBBB (79 mA h g^{-1}), we seek to develop higher capacity derivatives of DBBB by removing or minimizing substituent groups. The remarkable performance and durability of DBBB stems from its elegant chemical structure and can be attributed to: (1) the aromaticity of the dimethoxybenzene platform (Hückel's rule) which helps stabilize the radical cation;[17] (2) the bulky *tert*-butyl groups that provide both electron donating and steric protection effects to further stabilize the radical cation;[18] (3) the symmetry of the di-*tert*-butyl-dimethoxybenzene redox core.[12,19] To reduce the molecular weight without sacrificing electrochemical performance, two modifications are contemplated. First, given that the two *tert*-butyl groups contribute ~34% of DBBB's molecular mass, replacing these bulky groups will lead to the immediate reduction in molecular weight. As the smallest electron donating group that still provides some measure of steric protection, methyl groups appear to be a good choice. Second, the long ether chains on the DBBB molecule facilitate solubilization into polar solvents but are bulky (37% of the molecular weight) and do not influence the electrochemical performance. However, with the removal of the non-polar *tert*-butyl groups, these ether chains may not be necessary for acceptable solubility. Thus, based on these design considerations, a family of dimethoxybenzene derived molecules including 2-methyl-1,4-dimethoxybenzene (MDB), 23DDB, 25DDB, and 2,6-dimethyl-1,4-dimethoxybenzene (26DDB), has been proposed. Details about the material availability and synthesis procedures can be found in the ESI.† As 1,4-dimethoxybenzene (DB) is known to undergo irreversible electro-oxidation,[20] methyl groups were gradually introduced onto the benzene ring to provide additional stabilization effects in order to construct electrochemical reversible systems.

While all of the derivative molecules are significantly smaller than DBBB (>50% lower molecular weight) and of similar molecular structure, their electrochemical performances are quite different. As the smallest molecule in this study, MDB displayed poor chemical reversibility, likely due to the insufficient stabilization effect of the single methyl group (Fig. S1 in the ESI†). For the dual methyl substituted compounds, the electrochemical behavior is strongly associated with the methyl group locations on the benzene ring. For example, regardless of the presence of two methyl groups on the benzene ring, 26DDB still exhibits an irreversible behavior based on the cyclic voltammetry results (Fig. S2 in the ESI†). However, when the two methyl groups were introduced on 2,3- or 2,5-positions, the cyclic voltammograms of the 23DDB and 25DDB molecules show well defined symmetric reduction and oxidation features comparable to DBBB (Fig. 2). Furthermore, the location of the methyl groups appears to have a minor impact on the redox potential as the redox potential of 25DDB is similar to that of DBBB, a slight, positive shift was observed for 23DDB. Cyclic voltammetry results indicate that the modifications on the bulky moieties of DBBB, such as removing ether chains and replacing the *tert*-butyl groups with methyl groups, do present a possible pathway to construct chemically reversible molecules with reduced molecular weight but comparable electrochemical response. The gravimetric capacity of 23DDB and 25DDB (161 mA h g^{-1}) is more than twice that of DBBB (79 mA h g^{-1}) due to the decreased molecular weight (166 g mol^{-1} *vs.* 338 g mol^{-1}). These materials appear to approach the minimal substitution requirements necessary to stabilize 1,4-dimethoxybenzene based structures and thus represent the upper capacity limit for this family of single electron transfer molecules.

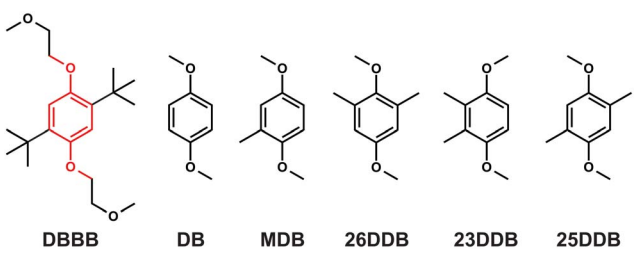

Fig. 1 Molecular structures of 2,5-di-*tert*-butyl-1,4-bis(2-methoxyethoxy)benzene (DBBB), 1,4-dimethoxybenzene (DB), 2-methyl-1,4-dimethoxybenzene (MDB), 2,6-dimethyl-1,4-dimethoxybenzene (26DDB), 2,3-dimethyl-1,4-dimethoxybenzene (23DDB), and 2,5-dimethyl-1,4-dimethoxybenzene (25DBB).

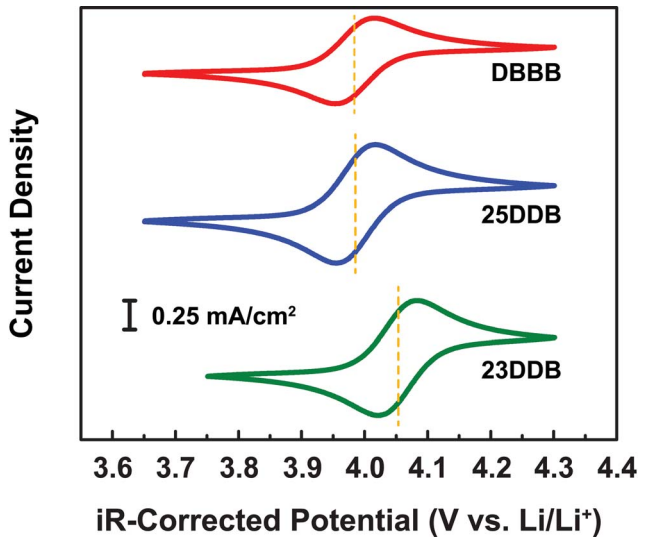

Fig. 2 Cyclic voltammograms of 2,5-di-*tert*-butyl-1,4-bis(2-methoxyethoxy)benzene (DBBB), 2,5-dimethyl-1,4-dimethoxybenzene (25DDB), 2,3-dimethyl-1,4-dimethoxybenzene (23DBB). All electrolytes consisted of 10 mM active species in 0.5 M LiTFSI/PC. The working, reference, and counter electrodes are glassy carbon electrode, fritted lithium metal, and unfritted lithium metal, respectively. The scan rate is 0.02 V s^{-1}.

Quantitative analysis of cyclic voltammograms over a range of scan rates are used to determine electrochemical and mass transfer parameters for DBBB, 23DDB, and 25DDB. The cyclic voltammograms and corresponding Randles–Sevick plots can be found in the ESI (Fig. S3†). The results of these analyses are summarized in Table 1. For comparison, the characteristics of ferrocene, a well-studied standard reference compound for non-aqueous systems,[21] are reported in the same electrolyte. As described above, the half-wave potentials ($E_{1/2} = (E_{pa} + E_{pc})/2$, also known as the redox potential) for DBBB and 25DDB are practically identical whereas 23DDB is about 50 mV more positive. All molecules demonstrated similar redox reversibility with peak separations ($\Delta E = E_{pa} - E_{pc}$) near the theoretical 0.059 V (at 25 °C) associated with a Nernstian, one-electron transfer couple. The peak separation for all four compounds showed a slight dependence on scan rate (from 0.005 to 0.1 V s^{-1}). The diffusion coefficients of DBBB, 23DDB, and 25DDB are estimated as 1.24×10^{-6}, 2.24×10^{-6}, 2.43×10^{-6} cm^2 s^{-1}, respectively. The diffusion coefficients of 23DDB and 25DDB are roughly twice that of DBBB, as predicted by the Stokes–Einstein relationship,[22] highlighting an advantage of smaller redox active compounds. Chemical reversibility is determined by studying the cathodic discharge/anodic charge (Q_{red}/Q_{ox}) ratios. All three compounds show minor non-idealities in chemical reversibility given the time scale of a CV experiment, but no scan rate dependence was observed. While the primary source of this deviation is likely the instability of the oxidized radical ions, irreversible electrolyte oxidation, especially at high electrode potentials, may also contribute to the charge imbalance. By comparison, ferrocene showed near complete charge retention (0.999 ± 0.001) though it is important to note this occurs at a lower voltage well within the electrolyte stability window.

In addition to increased gravimetric capacity and diffusivity, 23DDB and 25DDB demonstrate higher solubility than DBBB. The room temperature solubility of DBBB in 0.5 M LiTFSI/PC is *ca.* 0.3 M,[23] while in the same electrolyte the solubility of 23DDB and 25DDB are 2.0 M and 0.6 M, respectively. As discussed earlier, this enhanced solubility can be partially attributed to the absence of bulky non-polar *tert*-butyl groups. However, the dramatic increase in 23DDB's solubility may be due to its asymmetric structure which increases the intramolecular dipole moments resulting in greater intermolecular interactions between the active species and the polar solvent (PC). We note that the solubility of the redox molecules in their charged state is equally important for successful flow battery operation. Detailed quantification of solubility as a function of state-of-charge and various electrolyte solutions will be the subject of future work.

Building on the CV results, 23DDB, 25DDB, and DBBB are further evaluated by galvanostatically cycling in a bulk electrolysis cell which enables characterization of redox species' stability over multiple charge and discharge cycles. An electrolyte comprised on 1 mM active species in 0.5 M LiTFSI/PC was cycled at a charge/discharge current of 0.402 mA (0.5 C rate) between 0 and 50% SOC for 100 cycles. Note that the theoretical capacity of DBBB, 23DDB, and 25DDB are 79.2 mA h g^{-1}, 161.4 mA h g^{-1} and 161.4 mA h g^{-1}, thus 50% SOC for each are 39.6 mA h g^{-1}, 80.7 mA h g^{-1}, and 80.7 mA h g^{-1} (Fig. 3). The upper and lower cut-off voltages were set at *ca.* 150 mV above and below the redox potential established by cyclic voltammetry. Representative voltage profiles for all three compounds for the first 10 cycles and the last 10 cycles are shown in Fig. 4. Due to the low currents and high stirring rate, iR contributions were minimal leading to high voltage efficiencies (~99%) for all three

Table 1 A summary of electrochemical properties obtained from cyclic voltammetry of DBBB, 25DDB, 23DDB, and ferrocene. The experimental conditions are identical as those in Fig. 2. $E_{1/2}$ is the half-wave potential. $E_{pa} - E_{pc}$ is the peak separation. D_{red} and D_{ox} are diffusion coefficients of the reduced and oxidized species, respectively. Q_{red}/Q_{ox} is the charge ratio of the reduction process to the oxidation process. All experiments were performed in triplicate

	$E_{1/2}$ V	$E_{pa} - E_{pc}$ V	$D_{red} \times 10^{-6}$ cm^2 s^{-1}	$D_{ox} \times 10^{-6}$ cm^2 s^{-1}	Q_{red}/Q_{ox} —
DBBB	3.985 ± 0.001	0.062 ± 0.001	1.241 ± 0.040	1.202 ± 0.037	0.977 ± 0.007
25DDB	3.983 ± 0.001	0.061 ± 0.001	2.427 ± 0.170	2.385 ± 0.170	0.975 ± 0.008
23DDB	4.039 ± 0.007	0.062 ± 0.001	2.243 ± 0.033	2.156 ± 0.005	0.964 ± 0.014
Ferrocene	3.299 ± 0.001	0.060 ± 0.001	2.283 ± 0.030	2.291 ± 0.029	0.999 ± 0.001

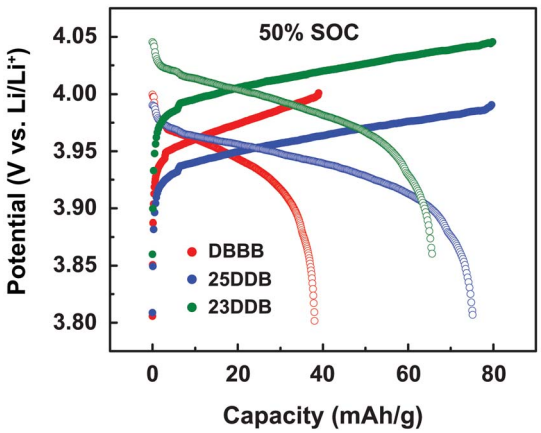

Fig. 3 Representative charge (solid circle)/discharge (open circle) cycles of DBBB (red), 25DDB (blue), and 23DDB (green) at 0.5 C from 0 to 50% state of charge in a bulk electrolysis cell. All electrolytes consisted of 1 mM active species in 0.5 M LiTFSI/PC and a total solution volume of 30 mL.

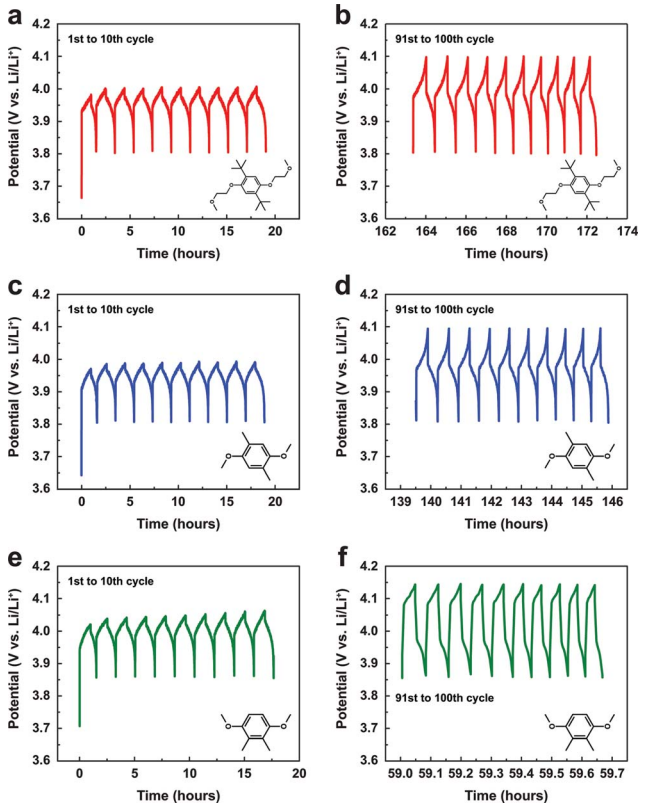

Fig. 4 Cycling profiles of DBBB (red), 25DDB (blue), and 23DDB (green) at 0.5 C from 0–50% state of charge for 1st to 10th cycle (a, c, e) and 91st to 100th cycle (b, d, f) in a bulk electrolysis cell. All electrolytes consisted of 1 mM active species in 0.5 M LiTFSI/PC and a total solution volume of 30 mL.

compounds. In the first 10 cycles, the charge/discharge behavior of all compounds is similar although the voltage profiles of 23DDB start to evolve (steeper slopes) from the 8th cycle. All compounds reach the 50% SOC before the upper cut-off voltages. For the last 10 cycles, the voltage profiles have significantly changed with all compounds reaching the upper and lower cut-off voltages. Furthermore, while the behavior of DBBB and 25DDB are similar, significant resistance (*ca.* 0.1 V) appeared in 23DDB voltage profiles resulting in shortened charge/discharge curves (Fig. 4f).

The charge/discharge capacities and the corresponding coulombic efficiency plots for DBBB, 23DDB, and 25DDB are shown in Fig. 5a and b, respectively. Fig. 5a shows the charge and discharge capacity of each compound over 100 cycles. The capacity decay from the theoretical 50% SOC over time reflects the degradation of radical intermediates. Specifically, under these experimental conditions, 50% DBBB was converted to non-rechargeable species after 75 ± 4 cycles whereas it took 48 ± 4 and 15 ± 1 cycles to irreversibly consume 50% 25DDB and 23DBB, respectively. DBBB shows the best capacity retention, which can be explained by the finely-tuned molecular structure (discussed above). Compared to DBBB, the 25DDB does not show as stable performance but still outperforms its asymmetric isomer 23DDB. This observation is consistent with previous studies, which showed the symmetric molecular structures tend to exhibit higher electrochemical stability as compared to their asymmetric counterparts.[11,12,19] The less stable performance of 23DDB is consistent with the abnormal voltage profiles observed in Fig. 4f, and it is believed that the significant resistance is related to the decomposition of 23DDB during cycling. However, a more rigorous evaluation of the stability of 23DDB is required for conclusive assessments. Detailed studies of the stability of a series of substituted alkoxybenzene-based redox active compounds and the corresponding degradation pathways *via* coupled electrochemical and electron paramagnetic resonance (EPR) methods is ongoing and will be reported in due course.

Fig. 5b shows the coulombic efficiencies (CE) of DBBB, 23DDB and 25DDB prior to the start of charge capacity decay. Note that the first cycle efficiency of all three compounds is significantly lower than subsequent cycles. This is likely due to the initial interfacial reactions that are typical to thermodynamically unstable systems and are comparable to the solid-electrolyte interphase (SEI) formation in Li-ion batteries.[10,13] Note that the frit separating the lithium metal counter electrode chamber and the working electrode chamber is not ion-selective thus some species crossover is expected. However, this is expected to have a similar impact on all of the compounds tested. After the first cycle, the average CEs of DBBB and 25DDB are >90% with DBBB being slightly higher, whereas the 23DDB is significantly lower at *ca.* 75–80%. These observations are in line with the capacity retention curves as well as with the CV data shown in Table 1.

In summary, we report on the development and electrochemical performance of a series of substituted 1,4-dimethoxybenzene derivatives. In particular, our goal was to improve the gravimetric capacities of the redox active molecules without sacrificing performance while imparting other favorable properties. Two promising derivatives, 25DDB and 23DDB, have been developed by reducing the substituent groups of DBBB, such as the *tert*-butyl groups and ether chains. As a result both molecules not only demonstrated desirable electrochemical

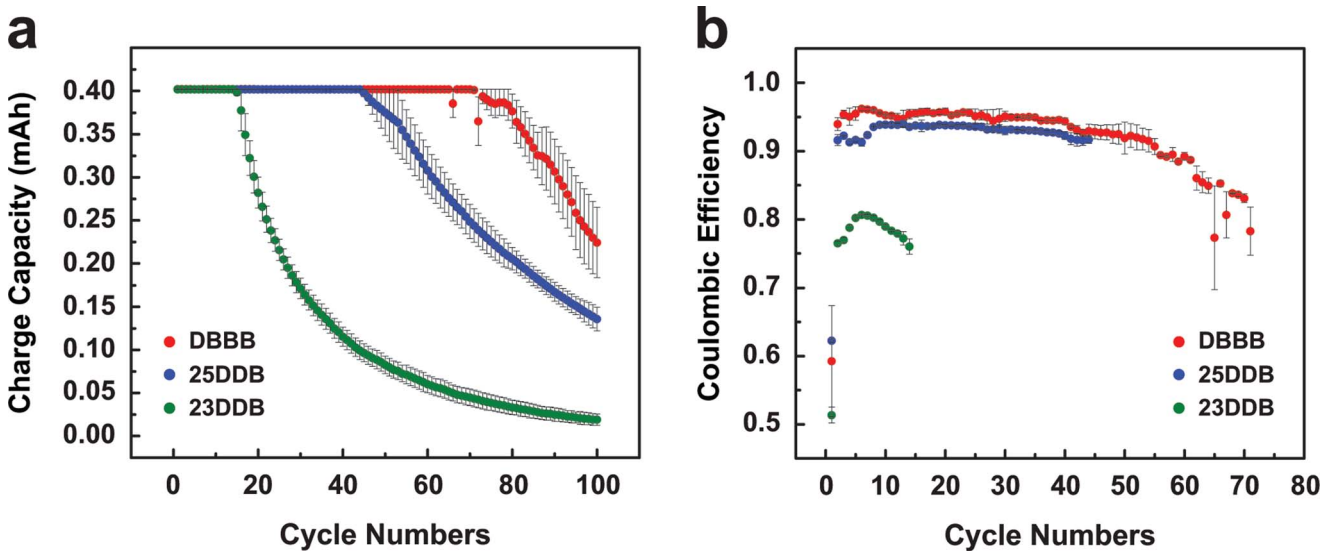

Fig. 5 (a) Charge capacity profiles for DBBB (red), 25DDB (blue), and 23DDB (green) with respect to the cycle number based on the data from Fig. 4. (b) Coulombic efficiencies of the plateaued region on the corresponding capacity profile. Data shown represents the average of two independent experiments for each compound.

and physical characteristics, but achieve these at about half the molecular weight of the parent compound, resulting in a marked enhancement in gravimetric capacity (161 mA h g^{-1}). Further, given the small size of these molecules, additive strategies may be employed to enhance the long-term cycle stability while maintaining high capacities. Consequently, both 23DDB and 25DDB are promising materials for non-aqueous RFBs. Future studies will focus on translating these tailored molecules into high concentration redox electrolytes and evaluating the performance and durability of non-aqueous flow cells based on these chemistries.

Acknowledgements

This work was supported as part of the Joint Center for Energy Storage Research, an Energy Innovation Hub funded by the U.S. Department of Energy, Office of Science, Basic Energy Sciences. The submitted manuscript has been created by UChicago Argonne, LLC, Operator of Argonne National Laboratory ("Argonne"). Argonne, a U.S. Department of Energy Office of Science Laboratory, is operated under Contract no. DE-AC02-06CH11357. DBBB, also referred to as ANL-2, was synthesized by Krzysztof Pupek and Trevor Dzwiniel at Argonne's Materials Engineering Research Facility and was funded by DOE-EERE Office of Vehicle Technologies. J.H. and L.S. contributed equally to this work. We thank Lei Cheng (ANL) for stimulating discussion.

Notes and references

1 B. Dunn, H. Kamath and J.-M. Tarascon, *Science*, 2011, **334**, 928–935.
2 Z. Yang, J. Zhang, M. C. W. Kintner-Meyer, X. Lu, D. Choi, J. P. Lemmon and J. Liu, *Chem. Rev.*, 2011, **111**, 3577–3613.
3 G. H. A. A. Akhil, A. B. Currier, B. C. Kaun, D. M. Rastler, S. B. Chen, A. L. Cotter, D. T. Bradshaw and W. D. Gauntlett, *DOE/EPRI 2013 Electricity Storage Handbook in Collaboration with NRECA*, SANDIA REPORT, SAND2013–5131, 2013.
4 R. M. Darling, K. G. Gallagher, J. A. Kowalski, S. Ha and F. R. Brushett, *Energy Environ. Sci.*, 2014, **7**, 3459–3477.
5 ARPA-E, Grid-Scale Rampable Intermittent Dispatchable Storage, 2015, http://www.arpa-e.energy.gov/?q=arpa-e-programs/grids.
6 George Crabtree, 2014.
7 Q. H. Liu, G. M. Grim, A. B. Papandrew, A. Turhan, T. A. Zawodzinski and M. M. Mench, *J. Electrochem. Soc.*, 2012, **159**, A1246–A1252.
8 R. M. Darling and M. L. Perry, *J. Electrochem. Soc.*, 2014, **161**, A1381–A1387.
9 B. Huskinson, M. P. Marshak, C. Suh, S. Er, M. R. Gerhardt, C. J. Galvin, X. Chen, A. Aspuru-Guzik, R. G. Gordon and M. J. Aziz, *Nature*, 2014, **505**, 195–198.
10 K. Xu, *Chem. Rev.*, 2004, **104**, 4303–4418.
11 F. R. Brushett, J. T. Vaughey and A. N. Jansen, *Adv. Energy Mater.*, 2012, **2**, 1390–1396.
12 L. Zhang, Z. Zhang, P. C. Redfern, L. A. Curtiss and K. Amine, *Energy Environ. Sci.*, 2012, **5**, 8204–8207.
13 J. Huang, L. Cheng, R. S. Assary, P. Wang, Z. Xue, A. K. Burrell, L. A. Curtiss and L. Zhang, *Adv. Energy Mater.*, 2015, **5**, 1401782.
14 X. Wei, W. Xu, J. Huang, L. Zhang, E. Walter, C. Lawrence, M. Vijayakumar, W. A. Henderson, T. Liu, L. Cosimbescu, B. Li, V. Sprenkle and W. Wang, *Angew. Chem., Int. Ed.*, 2015, DOI: 10.1002/anie.201501443.
15 J. Huang, I. A. Shkrob, P. Wang, L. Cheng, B. Pan, M. He, C. Liao, Z. Zhang, L. A. Curtiss and L. Zhang, *J. Mater. Chem. A*, 2015, **3**, 7332–7337.

16 J. Huang, N. Azimi, L. Cheng, I. A. Shkrob, Z. Xue, J. Zhang, N. L. Dietz Rago, L. A. Curtiss, K. Amine, Z. Zhang and L. Zhang, *J. Mater. Chem. A*, 2015, **3**, 10710–10714.
17 Z. Chen, Y. Qin and K. Amine, *Electrochim. Acta*, 2009, **54**, 5605–5613.
18 J. Chen, C. Buhrmester and J. R. Dahn, *Electrochem. Solid-State Lett.*, 2005, **8**, A59–A62.
19 Z. Zhang, L. Zhang, J. A. Schlueter, P. C. Redfern, L. Curtiss and K. Amine, *J. Power Sources*, 2010, **195**, 4957–4962.
20 Z. Chen, Q. Wang and K. Amine, *J. Electrochem. Soc.*, 2006, **153**, A2215–A2219.
21 R. R. Gagne, C. A. Koval and G. C. Lisensky, *Inorg. Chem.*, 1980, **19**, 2854–2855.
22 W. M. Deen, *Analysis of Transport Phenomena*, Oxford University Press, 2011.
23 L. Su, M. Ferrandon, J. A. Kowalski, J. T. Vaughey and F. R. Brushett, *J. Electrochem. Soc.*, 2014, **161**, A1905–A1914.